The Reduction of 1.06-μm Emission in a Double Cladding Tellurite All-solid Photonic Bandgap Fiber Doped with Neodymium Ions

Tong Hoang Tuan, Kohei Suzaki, Nobuhiko Nishiharaguchi, Takenobu Suzuki and Yasutake Ohishi
Toyota Technological Institute, 2-12-1 Hisakata, Tempaku-ku, Nagoya, 468-8511, Japan

Keywords: Neodymium Doped Fiber, All-solid Photonic Bandgap Fibers, Tellurite Fibers, Fiber Fabrication.

Abstract: In order to take advantage of the 1.33-μm emission from $^4F_{3/2}\rightarrow^4I_{13/2}$ transition of Nd^{3+} ions to realize many potential applications in this telecommunication band, it is important to filter out the intense 1.06-μm emission from the $^4F_{3/2}\rightarrow^4I_{11/2}$ transition. In this work, a new tellurite all-solid photonic bandgap fiber with double cladding layer was proposed. In addition, 8 high-index rods and an Nd^{3+}-doped core were arranged in a horizontal line and located in the center of the fiber. Numerical calculation was carried out to study the properties of the propagation modes at 0.8, 1.06 and 1.33 μm. By controlling the diameters of the core and high-index rods, it is possible to reduce the intensity of the 1.06-μm light, but maintain the intensity of the lights at 0.8 and 1.33 μm when they propagate in the fiber core.

1 INTRODUCTION

In recent years, the demands of optical amplifiers and lasers which can operate at various wavelengths in telecommunication bands to develop broadband optical systems for global telecommunication are rapidly raising. By using Erbium-doped fiber amplifiers (EDFA) as gain media for wavelength division multiplexing (WDM) systems, gain bandwidths from 1530 to 1560 nm (Jose, 2015) can be achieved but they are as narrow as 30 nm.

Among several active rare-earth ions that have been investigated for optical fiber amplifiers and lasers in the telecommunication band, Neodymium ion (Nd^{3+}) is an attractive candidate as 1.3-μm optical amplification active ions due to its $^4F_{3/2}\rightarrow$ $^4I_{13/2}$ transition (Miniscalco, 1988; Wang, 1994; Naftaly, 2000). However, when it is excited by pumping at 0.8 μm, the presence of the intense amplified spontaneous emission (ASE) at 1.06 μm has become a major problem. This ASE is attributed to the $^4F_{3/2}\rightarrow^4I_{11/2}$ transition whose branching ratio is about 5 times larger than that of the $^4F_{3/2}\rightarrow^4I_{13/2}$ transition for the ASE at 1.33 μm. To take full advantage of the 1.33-μm ASE, it is necessary to filter out the intense 1.06-μm ASE by using a continuous distributed filter (Naftaly, 2000).

In this work, we proposed a new tellurite all-solid photonic bandgap fiber (ASPBF) as a promising solution. The fiber consists of an Nd^{3+}-doped core in the center, a horizontal line of 8 high-index rods and double cladding layers. The propagation of the lights at 0.8, 1.06 and 1.33 μm in the fiber core was investigated. By controlling the fiber parameters, the transmission of the 1.06-μm light can be reduced and becomes weaker as compared to the others.

2 MATERIAL PROPERTIES

A conventional ASPBF usually consists of an arrangement of isolated high-index rods located in a low-index cladding (Knight, 2006). In this work, a step-index cladding profile was designed by using two cladding layers with different refractive index. The materials for the core, rod, inner cladding and outer cladding were developed by using tellurite glasses. The core material was TeO_2-ZnO-Na_2O-La_2O_3 which was doped with 0.5 wt% of Nd^{3+} ions (TZNL-Nd-doped). The tellurite glass TeO_2-Li_2O-WO_3-MoO_3-Nb_2O_5 (TLWMN) was used for high index rods and the TeO_2-ZnO-Na_2O-La_2O_3 (TZNL) and TeO_2-ZnO-Li_2O-K_2O-Al_2O_3-P_2O_5 glasses were used for the cladding materials, respectively. High purity TeO_2 powder (99.999%) and an electric furnace with dry gas flows of argon and oxygen were used to avoid the OH-contamination. After

Tuan, T., Suzaki, K., Nishiharaguchi, N., Suzuki, T. and Ohishi, Y.
The Reduction of 1.06-m Emission in a Double Cladding Tellurite All-solid Photonic Bandgap Fiber Doped with Neodymium Ions.
DOI: 10.5220/0007957302650268
In *Proceedings of the 16th International Joint Conference on e-Business and Telecommunications (ICETE 2019)*, pages 265-268
ISBN: 978-989-758-378-0

Table 1: Fitted Sellmeier coefficients for tellurite glasses TLWMN, TZNL-Nd-doped-0.5, TZNL and TZLKAP.

	A_1	A_2	B_1	B_2
TLWMN	3.2604	1.5796	190.0044	12704.1262
TZNL-Nd-doped-0.5	2.9259	0.0000	181.3663	31152.5524
TZNL	2.8614	0.0000	182.6837	7727.8810
TZLKAP	1.5729	2.3188	118.0236	18278.9797

quenching to room temperature, glass samples were cut into 1-mm-thick glass slides and polished carefully for the measurement of transmission and refractive index.

Transmission spectra of TLWMN (high-index rod material) and TZNL (inner cladding materials) were measured by an UV/VIS/NIR Spectrometer (Perkin Elmer, Lambda 900) and an FT-IR spectrometer (Perkin Elmer, Spectrum 100) and plotted in Fig. 1. Both TLWMN and TZNL glasses have high transmittance more than 70% covering a wide range from 0.5 to 5.0 µm. In addition, the transmission range of TZNL glass can extend up to 6.0 µm.

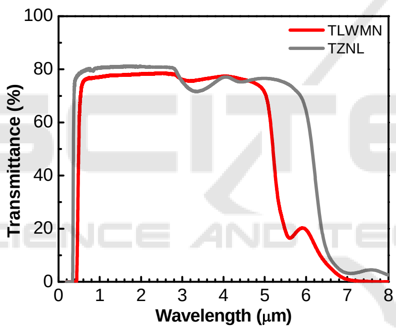

Figure 1: Measured transmission spectra of TLWMN and TZNL glasses.

The refractive indices of tellurite glasses at four wavelengths 633, 974, 1320 and 1544 nm were measured by a prism coupler system (Metricon 2010). They were fitted to Sellmeier equation as given in Eq. (1) in which A_1, A_2, B_1 and B_2 are Sellmeier coefficients and are shown in Table 1.

$$n=\sqrt{1+\frac{A_1\lambda^2}{\lambda^2-B_1^2}+\frac{A_2\lambda^2}{\lambda^2-B_2^2}} \quad (1)$$

The wavelength dependent refractive indices of TLWMN, TZNL-Nd-doped-0.5, TZNL and TZLKAP tellurite glasses obtained from Eq. (1) were used to calculate the light propagation and bandgap properties of the fiber by the Comsol Multiphysics software.

3 NUMERICAL CALCULATION AND DISCUSSION

A schematic image of the fiber structure was plotted in Fig. 2. The fiber was designed with an outer circular cladding (Clad 2) made of the TZLKAP glass and an inner hexagonal cladding (Clad 1) made of the TZNL glass. Inside the Clad 1, a solid rod of the TZNL-Nd-doped-0.5 was placed at the center as the fiber core and it was horizontally surrounded by two sets of 4 high index rods made of the TLWMN glass. The core diameter and the rod diameter were D_{core} and D_{rod}, respectively. The filling fraction (FF) is defined by the ratio between the rod diameter and the distance between two adjacent rods (p) as given in Eq. (2). The numerical technique Finite Element Method (FEM) and the perfectly match layer boundary condition were used. The size of the mesh was automatically optimized to maintain the calculation accuracy but reduce the calculation time. In the center of the fiber, the mesh was as small as 0.0018 µm. The size of the mesh became larger at the outer cladding and was as large as 0.9 µm. The mesh distribution for the calculation was schematically plotted in Fig. 2.

$$FF=\frac{D_{rod}}{p} \quad (2)$$

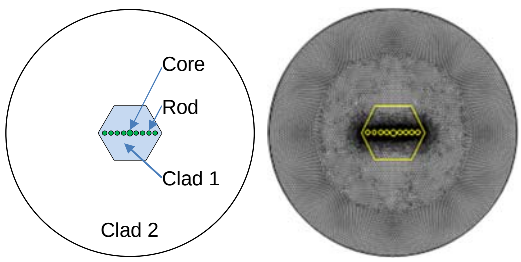

Figure 2: Schematic image of the fiber structure (left-side) and of the mesh distribution (right-side).

The target of this work is to realize fiber structures which allow high intensity lights to propagate in the core at 0.8 and 1.33 µm but hinder the transmission of the light at 1.06 µm. The calculation was first carried out when D_{core} was 3.0

µm, D_{rod} was 2.5 µm and *FF* was 0.75. Figure 3 shows the effective refractive index spectrum of the modes which can propagate in the core of the designed fiber in the vicinity of 0.8, 1.06 and 1.33 µm. The wavelength interval was 0.1 µm. At each wavelength, the red dot represents the fundamental mode or the mode which has highest intensity in the core. On the other hand, the blue dots show modes which were weakly confined in the core and their energy leak out to the surrounding region due to the photonic bandgap properties. It can be inferred that when the red dot overlaps with the blue dot, the light confinement in the core of that mode becomes weak. In other words, the intensity of the light which propagates in the core at that wavelength reduces. Provided that the red dot overlaps with the blue at 1.06 µm, the 1.06-µm ASE of Nd^{3+} ions will be weakly confined in the core, but the pump at 0.8 µm and the 1.33-µm ASE can still propagate in the core with high intensity if the red dot does not overlap the blue at 0.8 and 1.33 µm at the same time. That is to say, it is possible to filter out or reduce the 1.06-µm ASE continuously along the fiber as we expected by controlling the fiber parameters and the bandgap properties to satisfy the above conditions.

In order to confirm this feature, the intensity distribution of the mode fields which correspond to red dots at 0.8, 1.06 and 1.33 µm were calculated and shown in Figs. 3b, 3c and 3d. Because the red dots at those wavelengths do not coincide with the blue dots as can be seen in Fig. 3a, lights at those wavelengths are strongly confined in the core. Notably, the intensity of the light at 1.06 µm is about two times higher than that of the light at 1.33 µm as shown in Figs. 3c and 3d. It gives a chance for the 1.06-µm ASE to be dominant in the emission spectrum.

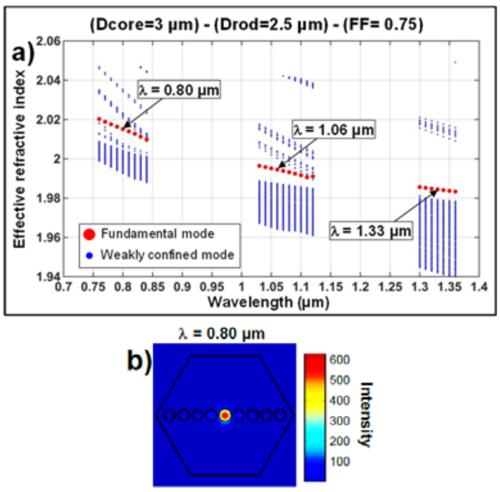

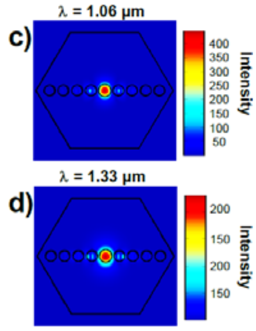

Figure 3: (a) Calculated effective refractive index of modes which can propagate in the fiber core when D_{core} was 3.0 µm, D_{rod} was 2.5 µm and *FF* was 0.75. (b), (c) and (d) are intensity distribution of modes which correspond to red dots at 0.8, 1.06 and 1.33 µm, respectively.

In order to investigate the effect of D_{rod}, similar calculations were done when it decreased from 2.5 µm to 2.3 µm and the results were shown in Fig. 4. Figure 4a shows that the red dot at 1.06 µm started to overlap the blue dot, but the red dots at 0.8 and 1.33 µm were still out of the blue dot range. In agreement with Fig. 4a, a Gaussian-like distribution of light intensity was recognized at 0.8 and 1.33 µm as shown in Figs. 4b and 4d, but it was not obtained at 1.06 µm as shown in Fig. 4c. Compared to the mode at 1.33 µm in Fig. 4d, the highest intensity of the mode at 1.06 µm in Fig. 4c becomes about 5 times lower. To put it another way, it is successful to reduce the intense 1.06-µm ASE but maintain the 1.33-µm ASE by using this ASPBF's structure.

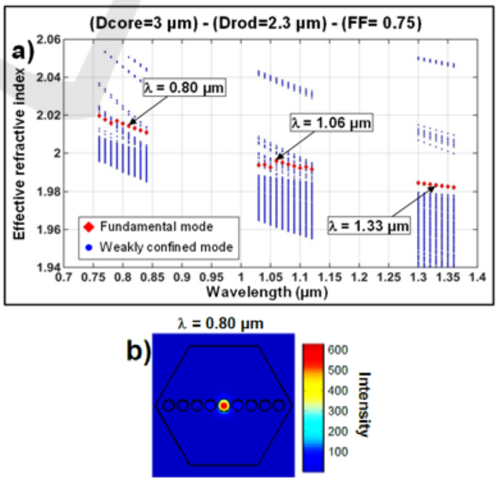

Figure 4: (a) Calculated effective refractive index of modes which can propagate in the fiber core when D_{core} was 3.0 µm, D_{rod} was 2.3 µm and *FF* was 0.75. (b), (c) and (d) are intensity distribution of modes which correspond to red dots at 0.8, 1.06 and 1.33 µm, respectively.

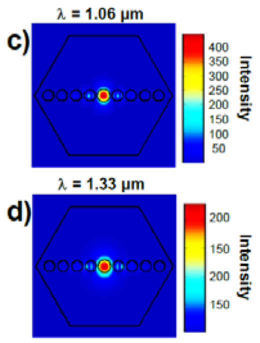

Figure 4: (a) Calculated effective refractive index of modes which can propagate in the fiber core when D_{core} was 3.0 µm, D_{rod} was 2.3 µm and *FF* was 0.75. (b), (c) and (d) are intensity distribution of modes which correspond to red dots at 0.8, 1.06 and 1.33 µm, respectively. (cont.)

When D_{core} decreases from 3.0 to 2.5 µm, the red dot at 1.06 µm moves deeper to the blue dot range as shown in Fig. 5a. Although the light at 1.06 µm can propagate in the core with a Gaussian-like distribution as shown in Fig. 5c, its highest intensity is about 3 times lower than that at 1.33 µm.

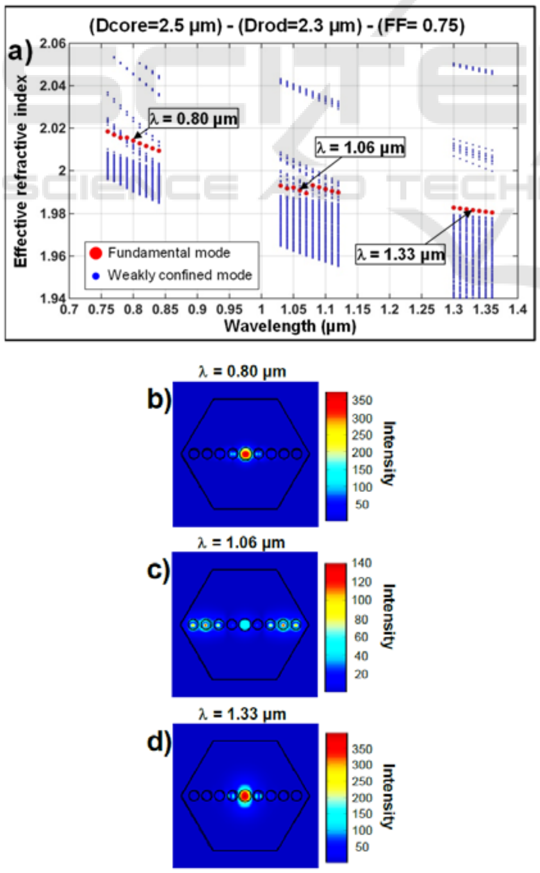

Figure 5: (a) Calculated effective refractive index of modes which can propagate in the fiber core when D_{core} was 2.5 µm, D_{rod} was 2.3 µm and *FF* was 0.75. (b), (c) and (d) are intensity distribution of modes which correspond to red dots at 0.8, 1.06 and 1.33 µm, respectively.

4 CONCLUSIONS

It was demonstrated in this work that by controlling fiber parameters of a new tellurite double-cladding ASPBF such as the filling fraction, the core and high-index rod diameters, the photonic bandgap properties were modified and the intense 1.06-µm emission peak due to the $^4F_{3/2} \rightarrow {}^4I_{11/2}$ transition of Nd^{3+} ions was greatly reduced as compared to the 1.33-µm ASE caused by the $^4F_{3/2} \rightarrow {}^4I_{13/2}$ transition. This feature is benefit to realize many potential applications employing the 1.3-µm emission of Nd^{3+} ions such as optical fiber amplifiers, display technologies, laser therapeutics and biomedical applications.

ACKNOWLEDGEMENTS

This work is supported by the Japan Society for the Promotion of Science (JSPS) KAKENHI (Grant Number 15H02250, 17K18891 and 18H01504) and the JSPS-CNRS joint research program.

REFERENCES

Jose, T. and Narayanan, V.,2015. Design of a gain flattened doped fiber amplifier with stabilized power output for WDM transmissions, *2015 International Conference on Microwave, Optical and Communication Engineering (ICMOCE)*, 193-196.

Miniscalco, W. J. and Andrews, L. J.,1988. Fiber Optic Lasers and Amplifiers for the Near-Infrared, *Mater. Sci. Forum*, 32-33, 501-510.

Wang, J. S., Vogel, E. M., Snitzer, E., Jackel, J. L., Dasilva, V. L. and Silberberg, Y., 1994. 1.3-µm emission of Neodymium and Praseodymium in Tellurite-based glasses, *J. Non-cryst. Solids*, 178, 109-113.

Naftaly, M. and A. Jha,2000. Nd^{3+}-doped fluoroaluminate glasses for a 1.3-µm amplifier, *J. Appl. Phys.*, 87, 2098-2104.

Knight, J. C., Luan, F., Pearce, G. J., Wang, A., Birks, T. A. and Bird, D. M.,2006. Solid photonic bandgap fibres and applications, *Jpn. J. Appl. Phys.*, 45, 6059-6063.